WIF1, a Wnt pathway inhibitor, regulates SKP2 and c-myc expression leading to G_1 arrest and growth inhibition of human invasive urinary bladder cancer cells

Yaxiong Tang,[1] Anne R. Simoneau,[1] Wu-xiang Liao,[3] Guo Yi,[2] Christopher Hope,[4] Feng Liu,[4] Shunqiang Li,[1] Jun Xie,[2] Randall F. Holcombe,[4] Frances A. Jurnak,[3] Dan Mercola,[5] Bang H. Hoang,[2] and Xiaolin Zi[1]

Departments of [1]Urology and [2]Orthopaedic Surgery and Chao Family Comprehensive Cancer Center and Departments of [3]Physiology & Biophysics, [4]Medicine, and [5]Pathology and Laboratory Medicine, University of California at Irvine, Irvine, California

Abstract

Epigenetic silencing of secreted wingless-type (Wnt) antagonists through hypermethylation is associated with tobacco smoking and with invasive bladder cancer. The secreted Wnt inhibitory factor-1 (WIF1) has shown consistent growth-inhibitory effect on various cancer cell lines. Therefore, we assessed the mechanisms of action of WIF1 by either restoring WIF1 expression in invasive bladder cancer cell lines (T24 and TSU-PR1) or using a recombinant protein containing functional WIF1 domain. Both ectopic expression of WIF1 and treatment with WIF1 domain protein resulted in cell growth inhibition via G_1 arrest. The G_1 arrest induced by WIF1 is associated with down-regulation of SKP2 and c-myc and up-regulation of p21/WAF1 and p27/Kip1. Conversely, reexpression of SKP2 in WIF1-overexpressing TSU-PR1 cells attenuated the WIF1-induced G_1 arrest. Furthermore, inhibition of nuclear Wnt signaling by either dominant-negative LEF1 or short hairpin RNA of TCF4 also reduced SKP2 expression. The human *SKP2* gene contains two TCF/LEF1 consensus binding sites within the promoter. Chromatin immunoprecipitation/real-time PCR analysis revealed that both WIF1 and dominant-negative LEF1 expression decreased the *in vivo* binding of TCF4 and β-catenin to the *SKP2* promoter. Together, our results suggest that mechanisms of WIF1-induced G_1 arrest include (*a*) SKP2 down-regulation leading to p27/Kip1 accumulation and (*b*) c-myc down-regulation releasing p21/WAF1 transcription. Additionally, we show that WIF1 inhibits *in vivo* bladder tumor growth in nude mice. These observations suggest a mechanism for transformation of bladder epithelium on loss of WIF1 function and provide new targets such as SKP2 for intervention in WIF1-deficient bladder cancer. [Mol Cancer Ther 2009;8(2):458–68]

Introduction

Muscle-invasive bladder cancer treatment requires a radical cystectomy or chemotherapy with radiation protocol (1). Radical cystectomy has many quality-of-life implications. In addition, the absolute survival benefit of neoadjuvant or adjuvant chemotherapy is debatable, and toxicity can be significant (2). Despite the current treatments, distant metastases eventually may develop in as many as 50% of patients with muscle-invasive tumors (2). Treatment options for metastatic bladder cancers are extremely limited, with a 5-year survival rate of ~6% and a median survival time of 12 to 20 months (2). Therefore, it is generally believed that there is an urgent need to expand the current paradigm of therapy by integrating novel targeted therapies for muscle-invasive bladder cancer.

The wingless-type (Wnt) pathway plays a central role in embryonic development, and aberrant activation of the Wnt pathway contributes to the progression of several major human cancers (3). Therefore, inhibition of Wnt effects has major therapeutic potential. Mutations of *APC* and *β-catenin* genes that are usually responsible for the deregulated Wnt/β-catenin pathway in other tumors (e.g., colon and liver cancers) are uncommon in human bladder cancer (4, 5). Instead, down-regulation of secreted Wnt antagonists by gene deletion or promoter hypermethylation (6–9) is frequently detected in human bladder cancer tissues and is a strong predictor of poor survival (6). In addition, the loss of secreted Wnt antagonists may play an etiologic role in tobacco smoking-related bladder cancer, as hypermethylation of secreted Wnt antagonists occurs more often in current and former smokers (8, 10, 11). Secreted Wnt antagonists, classified as secreted Frizzled-related protein family, Dickkopf family, and Wnt inhibitory factor-1 (WIF1), are negative modulators of Wnt signaling

Received 9/11/08; revised 11/4/08; accepted 11/8/08; published OnlineFirst 01/27/2009.

Grant support: NIH grants CA129793 and CA122558 and AICR grant 41493 (X. Zi), Neil Chamberlain Urological Cancer Research Fund (X. Zi and A.R. Simoneau), Cancer Research Coordinating Committee grant CRCC-35281 and University of California at Irvine CORCL MI-2002-2003-18 (F.A. Jurnak), NIH grant U01 CA114810-02 (D. Mercola), and NIH CA116003 (B.H. Hoang).

The costs of publication of this article were defrayed in part by the payment of page charges. This article must therefore be hereby marked *advertisement* in accordance with 18 U.S.C. Section 1734 solely to indicate this fact.

Note: Current address for S. Li: Department of Medicine, Washington University, 660 South Euclid Avenue, Campus Box 8056, St. Louis, MO 63110.

Requests for reprints: Xiaolin Zi, Department of Urology and Chao Family Comprehensive Cancer Center, Building 55, Room 302, 101 The City Drive South, Route 81, Orange, CA 92868. Phone: 714-456-8316; Fax: 714-456-2240. E-mail: xzi@uci.edu

doi:10.1158/1535-7163.MCT-08-0885

(12). Because WIF1 silencing due to promoter hypermethylation has been shown in a variety of cancers including colorectal, prostate, bladder, melanoma, lung, and other cancers (13–24), restoring WIF1 expression in cancer cells to study its biological function has been done by several groups (13–24). The commonly described effect of WIF1 on cancer cells is the inhibition of cancer cell growth (13–24). However, the underlying mechanisms for the inhibitory effect of WIF1 on tumor cell growth remain largely unknown.

The Wnt/β-catenin pathway has been shown to determine the proliferation/differentiation balance through its regulation of G_1-S transition in several cellular systems (e.g., stem, progenitor, and colorectal cancer cells; refs. 25, 26). The G_1-S transition in cell cycle is driven mainly by cyclin-dependent kinase (CDK) 2 that is controlled by abundance of CDK inhibitors: p21/WAF1 (p21) and p27/Kip1 (p27; ref. 27). The regulation of G_1-S transition is physiologically required for cell fate determination—a cell undergoing apoptosis, proliferation, or differentiation (27). However, during oncogenic transformation, G_1-S transition is deregulated by enhanced oncogenic growth signaling and/or by loss of tumor suppressors, which then leads to overgrowth of transformed cells (27). Some Wnts (e.g., Wnt1) have shown oncogenic activities in both mouse models and cell cultures (28). The activation of the Wnt/β-catenin pathway by Wnts elicits specific target genes (e.g., c-myc and cyclin D1) for cell cycle regulation and growth (25, 29). It is possible that the secreted Wnt antagonist WIF1 binds to specific Wnts and regulates the expression of cell cycle-related Wnt target genes for its growth-inhibitory effect on cancer cells. Therefore, the identification of WIF1-regulated Wnt target genes will provide important mechanism for transformation of bladder epithelium on loss of WIF1 function and provide new targets for intervention in WIF1-deficient bladder cancer.

In this study, we show that WIF1 binds to Wnt1 and inhibits the growth of invasive bladder cancer cell lines via induction of G_1 arrest. The G_1 arrest by WIF1 is associated with down-regulation of SKP2 and c-myc and up-regulation of p21 and p27. In addition, we provide the first evidence that SKP2, a substrate recognition component of Skp1-Cul1-F-box ubiquitin-ligase responsible for p27 protein abundance and a putative oncogene, is a potential target gene of the Wnt pathway.

Materials and Methods

Plasmids, Cell Lines, and Stable Transfection

The pRK5/WIF1-IgG plasmid, containing a full-length human *WIF1 Bam*HI-*Hin*dIII fragment and human IgG heavy chain, was a generous gift of Dr. Jen-Chih Hsieh (State University of New York at Stony Brook; ref. 12). Dominant-negative (DN) LEF1 expression construct DN-FL9Bneo was described previously in detail (30). The DNA fragment encoding human mature WIF1 domain (WD; amino acids 27-176; ref. 12) was amplified by PCR to create *Nco*I and *Hin*dIII sites at the 5′ and 3′ ends, respectively, and cloned behind the *trc* promoter of pPROEX HTb (Invitrogen), with its COOH terminus fused to 6× histidine affinity tag sequences. *pcDNA3-myc-SKP2* was obtained from Dr. Yue Xiong (University of North Carolina at Chapel Hill). Four independent short hairpin RNA (shRNA) constructs, targeting four different exons of *TCF4*, were purchased from SABiosciences. The human urinary bladder cancer T24 and TSU-PR1 cell lines, a mouse L cell line, and a mouse L cell line stably expressing mouse Wnt3a were obtained from the American Type Culture Collection. T24 and TSU-PR1 cells were maintained in McCoy's 5A medium and RPMI 1640, respectively. The NIH3T3 cell line stably expressing mouse Wnt1 was a generous gift of Dr. Andrew P. McMahon (Harvard University) and cultured in DMEM. T24 and TSU-PR1 cells at 60% confluency were transfected with *WIF1, DN-LEF1, pcDNA3-myc-SKP2, TCF4shRNA*, and control plasmids using FuGENE 6 (Roche). For stable transfection, transfected cells were selected with G418. Clones were selected expressing different levels of WIF1, DN-LEF1, and TCF4 and maintained in 500 μg/mL G418. All experiments were repeated using at least three different clones.

Fluorescence-Activated Cell Sorting Analysis for Cell Cycle Distribution

Cells were fixed in ice-cold 70% ethanol overnight and then stained in propidium iodide solution. Samples were analyzed on a BD FACScan flow cytometer and the percentage of cells in the S, G_0-G_1, and G_2-M phases of the cell cycle was determined using ModFIT software.

3-(4,5-Dimethylthiazol-2-yl)-2,5-Diphenyltetrazolium Bromide Assay

For evaluating the effect of WIF1, DN-LEF1, and TCF4shRNA expression on cell proliferation, T24 and TSU-PR1 cells stably transfected with WIF1, DN-LEF1, TCF4shRNA, or control pRK5 were cultured for 1, 3, and 5 days in 24-well plates. For studying the effects of recombinant WD protein on cell proliferation, T24 cells were treated with different concentrations of recombinant WD protein in 24-well plates for 2 days. The 3-(4,5-dimethylthiazol-2-yl)-2,5-diphenyltetrazolium bromide (Sigma) was added to a final concentration of 1 mg/mL. The reaction mixture was incubated for 3 h at 37°C and the absorbance was measured at 570 nm.

Soft Agar Colony Formation

Growth of TSU-PR1 cells transfected with human WIF1 or control vector in soft agar was assayed using 6-well plates. Each well contained 2 mL of 0.8% agar in complete medium as the bottom layer, 2 mL of 0.35% agar in complete medium and 1,000 cells as the feeder layer, and 2 mL complete medium as the top layer. Cultures were maintained under standard culture conditions. After 3 weeks, the number of colonies was determined with an inverted phase-contrast microscope at ×100 magnification where a group of >10 cells was counted as a colony. Crystal violet (0.1%) in methanol was used to stain the 6-well plates. After washing in PBS, colonies were photographed.

Protein Extraction, Conditioned Medium, and Western Blot

For membrane and cytosolic protein fractionation, cells were collected in TES resuspension buffer and homogenized on ice. The cytosolic fraction was recovered by ultracentrifugation and the membrane-enriched pellet was solubilized as described previously (30). For extraction of total proteins, cells were lysed in radioimmunoprecipitation assay buffer (30). Conditioned media were prepared by culturing TSU-PR1 stably transfected with vector control or *WIF1* in serum-free RPMI and by culturing mouse L cells, mouse L cells stably expressing Wnt3a, or NIH3T3 cells stably expressing Wnt1 in DMEM with 10% fetal bovine serum for 48 h. The conditioned medium from TSU-PR1 cell lines was concentrated 40 times by Centricon (Millipore). For Western blotting analysis, protein lysates or concentrated conditioned medium was resolved electrophoretically on 8% to 12% SDS-PAGE, transferred to nitrocellulose membranes, and probed with primary antibodies against following proteins: β-catenin (Upstate); GSK3β, phospho-GSK3β, and SKP2 (Cell Signaling); p21, p27, and c-myc (Calbiochem); and human IgG, cyclin D1, CDK2, Wnt1, and β-actin (Santa Cruz Biotechnology). The position of proteins was visualized with an enhanced chemiluminescence detection system (Amersham Bioscience).

Immunoprecipitation and Kinase Assay

For evaluating the WIF1/Wnt1 immunocomplex formation, concentrated conditioned medium was immunoprecipitated with protein A-agarose and anti-human IgG and probed with anti-Wnt1 antibody. For CDK2 kinase assays, protein lysates were subjected to immunoprecipitation in lysis buffer at 4°C overnight in the presence of anti-CDK2 antibody and protein A-agarose beads. Phosphorylation of histone H1 was measured by incubating the beads with 40 μL ''hot'' kinase solution for 30 min at 30°C (31). Samples were analyzed by 12% SDS-PAGE and the gels were dried and subjected to autoradiography.

Reverse Transcription-PCR and Real-time Reverse Transcription-PCR

Total RNA was isolated from TSU-PR1 cells using the RNAazol B method as described (31). Real-time reverse transcription-PCR was done as described previously (30) using a MyiQ real-time thermocycler (Bio-Rad). The PCR condition was as follows: 95°C for 5 min, 40 cycles of 30 s at 95°C, 30 s at 60°C, and 60 s at 72°C. Relative quantitative fold change compared with control was calculated using the comparative C_t method (27). C_t is the cycle number at which fluorescence intensity first exceeds the threshold level. ΔC_t is C_t (target gene) - C_t (actin). Gene-specific primer pairs (including product size) are available upon request. Specificity of amplification products were checked by melting curve analysis and agarose gel electrophoresis.

Chromatin Immunoprecipitation/Real-time PCR Assay

Cells (2×10^7) were cross-linked in a 1% formaldehyde solution, lysed, and sonicated to sheer chromatin to an average size of ~600 kb. The extract was immunoprecipitated with anti-TCF4 and anti-β-catenin antibodies, respectively. Anti-rabbit or anti-goat IgG antibody was used as a negative control. Then, DNA-protein cross-links were reversed by heating at 65°C for 4 h. A part of each captured immunocomplex was used for Western analysis to confirm that the captured chromatin contained the transcription factor corresponding to the specificity of the antibody that had been used for chromatin immunoprecipitation. The DNA fragments were purified for PCR and real-time PCR. DNA recovered from an aliquot of sheared chromatin was used as control (input). *SKP2* primer pairs for PCR were as follows: For TCF/LEF1 binding site 1, forward 5′-CCCAGGCCCCTTCTATAGTC-3′ and reverse 5′-CTCAGATGATCCACCCACCT-3′, PCR product size 227 bp. For TCF/LEF1 binding site 2, forward 5′-TTGCAATCTTCAGGGAAAGG-3′ and reverse 5′-GGCTAAGCCGTTCATCAAAC-3′, PCR product size 151 bp. Real-time reverse transcription-PCR was done as described above. The C_t values for the technical repeats show minimal variation within half a C_t value of each other. The C_t value for each sample was normalized to the input samples: ΔC_t [C_t (sample) - C_t (input)]. The enrichment of the chromatin immunoprecipitation target is expressed as a fold difference ($2^{-[\Delta Ct]}$). The PCR products generated from the chromatin immunoprecipitation template were sequenced, and the identity of the *SKP2* promoter was confirmed. Each chromatin immunoprecipitation was carried out at least three times with similar results.

Expression, Purification, and Refolding of the WD

The WD expression plasmid was transfected into *Escherichia coli* strain DH5α, and high-level expression of WD protein was induced by IPTG. The cells were lysed. The inclusion bodies were collected and resuspended in 50 mmol/L Tris-HCl (pH 8.0), 0.1 mmol/L EDTA, and 6 mol/L guanidine hydrochloride. For refolding, this suspension was incubated for 1 h at room temperature with constant stirring and then centrifuged. The solubilized WD and refolded WD were purified by nickel column with imidazole gradient elution (20-500 mmol/L) and gel filtration on HiLoad 16/60 Superdex 75 column (Amersham). Purified WD was subjected to SDS-PAGE to determine the concentration and Western analysis to verify the protein. Monoclonal anti-polyhistidine antibody (Sigma) and goat anti-mouse IgG (H + L)-AP conjugate (Bio-Rad) were used as primary and secondary antibodies, respectively. Recombinant ROR2 protein was prepared using the similar approach and used as a control for WD.

In vivo Tumor Model

NCR-*nu/nu* (nude) mice were obtained from Taconic. Cells from each stable line were concentrated to 2×10^6 per 200 μL and injected s.c. into the left flank of each mouse. Each group of a stable line contained 10 mice. Once xenografts became established, their sizes were measured every 5 days. The tumor volume was calculated by the formula: $0.5236\ L_1(L_2)^2$, where L_1 is the long axis and L_2 is the short axis of the tumor. All of the animal studies were approved by the Institutional Animal Care and Use Committee at University of California at Irvine.

Immunohistochemistry

Flank tumors from injected animals were fixed in formalin and sectioned (4 μm). Antigen retrieval was done using 10 mmol/L sodium citrate (pH 6.0) at 95°C for 15 min. Slides were incubated with anti-human WIF1 antibody at 1:50 dilution and then with a biotinylated secondary antibody. Staining was visualized using horseradish peroxidase-3,3′-diaminobenzidine Cell & Tissue Staining Kit (R&D Systems) according to the manufacturer's instructions. Slides were counterstained with hematoxylin and photographed using a light microscope. Negative control samples were exposed to a secondary antibody and stained.

Statistics

Comparisons of cell density, number of colonies, relative levels of mRNA expression, and relative levels of protein expression between the different transfections were conducted by using Student's *t* test. For tumor growth experiments, repeated-measures ANOVA was used to examine the differences in tumor size among different transfections, time points, and transfection-time interactions. Additional post-hoc testing was done to examine the differences in tumor size between vector control and other transfections at each time point by using conservative Bonferroni method. All statistical tests were two sided. $P < 0.05$ was considered statistically significant.

Results

Ectopic Expression of WIF1 in T24 and TSU-PR1 Cell Lines Results in a Decrease of Anchorage-Dependent and Anchorage-Independent Growth

T24 and TSU-PR1 cell lines lack endogenous WIF1 expression (determined by semiquantitative reverse transcription-PCR; data not shown). To study the potential biological effect of WIF1 on invasive bladder cancer cells, T24 and TSU-PR1 cells were stably transfected with the pRK5/WIF1-IgG plasmid. The selected stable clones expressed different levels of WIF1-IgG fusion protein as confirmed by Western analysis with anti-human IgG antibody. Data from a representative T24/WIF1 or TSU/WIF1 clone is shown (Fig. 1A). The vector control transfectants were named as T24/pRK5 and TSU/pRK5, respectively (Fig. 1A). In addition, Fig. 1A indicates the secretion of WIF1-IgG fusion protein into conditioned medium. The final concentrations of secreted WIF1-IgG protein from different clones were estimated to range from 13 to 122 ng/mL, made by comparison with the known concentrations of recombinant WD proteins (data not shown).

For anchorage-dependent growth, each transfected cell line was measured by the 3-(4,5-dimethylthiazol-2-yl)-2,5-diphenyltetrazolium bromide assay. Figure 1B shows that both T24 and TSU-PR1 clonal lines stably transfected with WIF1-IgG plasmid exhibit a lower growth rate than T24 and TSU-PR1 cells transfected with vector control pRK5 do (P values < 0.01, Student's t test). Because T24 cells cannot grow in soft agar or nude mice, we only examined the

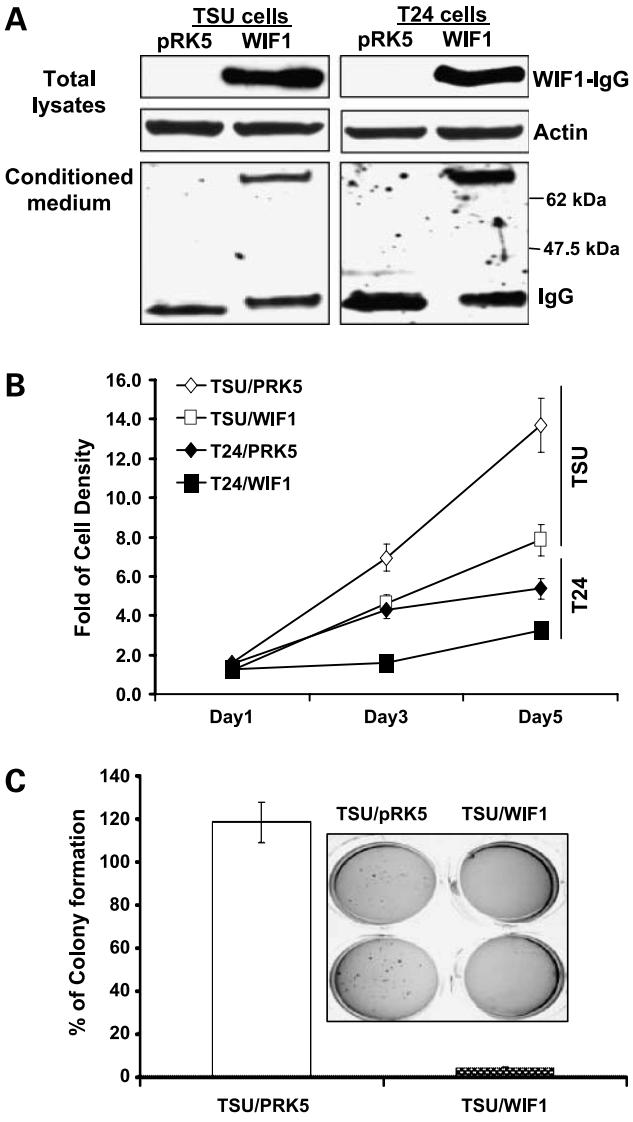

Figure 1. Ectopic expression of WIF1 in human urinary bladder cancer T24 and TSU-PR1 cells leads to a decrease of anchorage-dependent and anchorage-independent growth. **A,** WIF1 expression in cell lysates and conditioned medium of the representative stable transfectants was determined by Western blotting with anti-human IgG. **B,** cell proliferation assay in bladder cancer T24 and TSU-PR1cells expressing pRK5 vector control or WIF1 at 1, 3, and 5 d after cell seeding. **C,** qualitative (*inset*) and quantitative analyses of soft agar colony formation in TSU-PR1 cells expressing pRK5 vector control or WIF1. *Columns,* mean of four independent wells at optimum time of 21 d after the start of cell seeding; *bars,* SE.

anchorage-independent growth of each transfected TSU-PR1 clonal line. Figure 1C and *inset* show that the TSU-PR1 clonal line stably expressing WIF1 forms 95% fewer colonies in soft agar than TSU-PR1 cells transfected with vector control do ($P < 0.01$, Student's t test). However, we were unable to detect any polyADP-ribose polymerase cleavage (a hallmark for apoptosis) and an increase in pre-G_1 population by fluorescence-activated cell sorting analysis in all of those transfected cell lines, suggesting that

ectopic WIF1 expression did not cause significant apoptosis in T24 and TSU-PR1 cells (data not shown). These results suggest a biological role of WIF1 as a growth inhibitor during bladder carcinogenesis.

Ectopic Expression of WIF1 Induces G_1 Arrest in T24 and TSU-PR1 Cells Was Associated with Inhibition of Wnt1-Mediated Canonical Wnt Pathway

We next examined whether the cell growth-inhibitory effects of WIF1 expression were due to the perturbation in cell cycle progression. Figure 2A indicates a significant increase in the G_1 population in WIF1- versus pRK5-transfected T24 and TSU-PR1 cells. The G_1 populations in pRK5- or WIF1-transfected T24 and TSU-PR1 cells are 41% and 40% versus 53% and 61%, respectively ($P < 0.01$, Student's t test). The accumulation in the G_1 population by WIF1 expression was accompanied by a decrease of cell population in both S and G_2-M phases.

CDK2 is a major kinase responsible for G_1-S-phase transition during cell cycle progression (32). Consistent with the result of WIF1 expression inducing G_1 arrest, Fig. 2B shows a significant decrease in CDK2 activities in a WIF1 stable clone compared with vector control-transfected cells. Although there is no significant change in the protein level of CDK2 among the different clones, two major CDK2

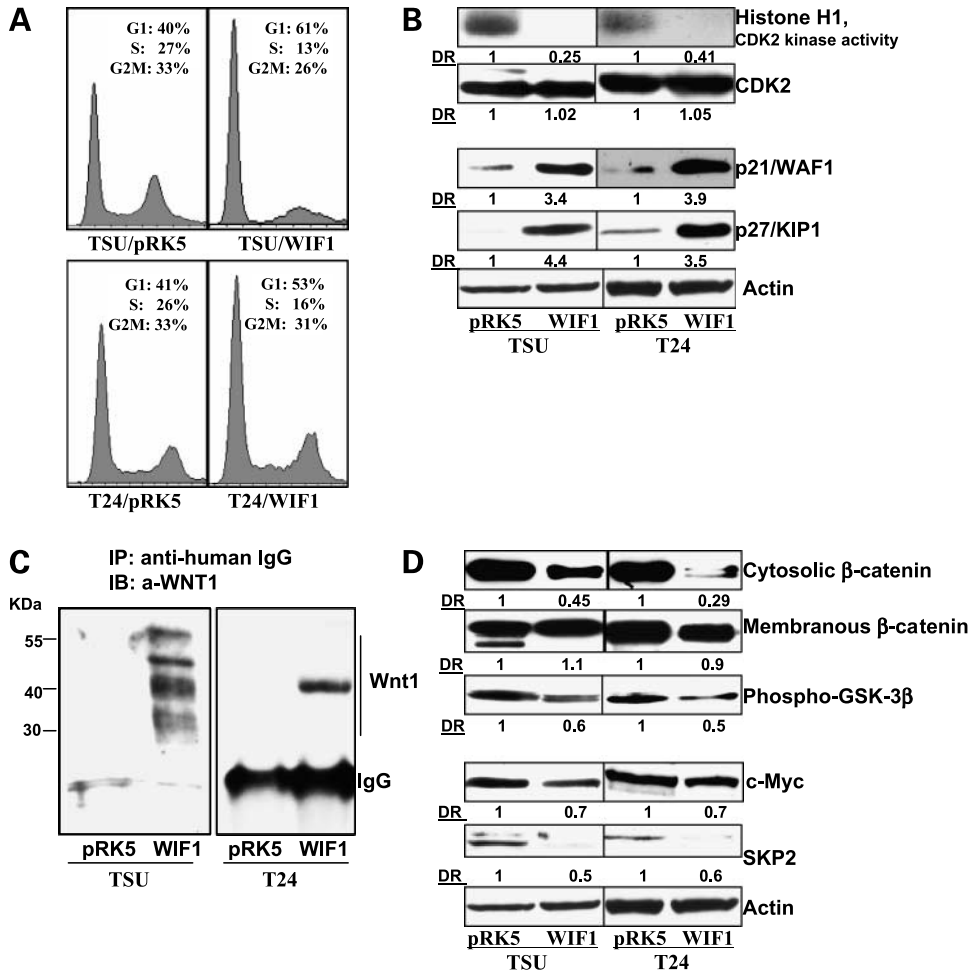

Figure 2. WIF1 induces G_1 arrest and inhibits the Wnt/β-catenin-mediated signaling pathway in T24 and TSU-PR1 cells. **A,** cell cycle distribution was analyzed by flow cytometry as detailed in Materials and Methods. Graphical presentation of percent cell cycle distribution in T24 and TSU-PR1 cells expressing pRK5 control or WIF1, respectively. Mean of three samples for each experiment. Results were similar in two independent experiments. **B,** histone H1-associated CDK2 kinase activity was determined in T24 and TSU-PR1 cells expressing pRK5 control or WIF1, respectively, as described in Materials and Methods. Western blotting analysis of p27/Kip1, p21/WAF1, and CDK2 in T24 and TSU-PR1 cells expressing pRK5 control or WIF1, respectively. Total protein lysates were used for SDS-PAGE and Western blotting. Membranes were detected by labeling with primary antibodies followed by addition of peroxidase-conjugated secondary antibody and visualized by ECL. The membrane was ''stripped'' and reprobed with anti-actin antibody for determination of protein loading. Representative of three independent experiments. **C,** immunoprecipitation assay of WIF1/Wnt1 complex. Concentrated conditioned medium from culturing T24 and TSU-PR1 cells expressing pRK5 control or WIF1 were incubated with anti-human IgG and protein A-agarose beads overnight at 4°C and probed with anti-Wnt1 antibody. Representative of three independent experiments in each case. **D,** Western blotting analysis of β-catenin, phospho-GSK3β, c-myc, and SKP2 protein expression in T24 and TSU-PR1 cells expressing pRK5 control or WIF1, respectively. Membranes were ''stripped'' and reprobed with anti-actin antibody for determination of protein loading control. Representative of three independent experiments. *DR,* densitometry measurement ratio relative to control treatment after adjusting for densities of β-actin loading control.

inhibitor proteins, p21 and p27, are significantly induced by ectopic expression of WIF1 (Fig. 2B). These results indicate the WIF1-promoted G_1 arrest is not likely due to a decrease in protein expression of the critical kinase CDK2 but is associated with significant increases in the CDK2 inhibitors: p21 and p27.

WIF1 was reported to bind *Drosophila* wingless, a homologue of human Wnt1 (12). Wnt1 has also been shown to bind to the extracellular domain of Ryk receptor that is homologous to WD (33). Thus, WIF1 may bind to Wnt1 via the WD to inhibit signaling. Figure 2C indicates that WIF1/IgG fusion protein forms an immunocomplex with endogenous Wnt1 in WIF1- but not pRK5-transfected TSU-PR1 and T24 cells. The multiple Wnt1 protein bands in TSU-PR1 cells suggest its modification by glycosylation and palmitoylation. Figure 2D shows that WIF1 overexpression causes a decrease in the protein levels of cytosolic β-catenin without evidently altering the level of membranous β-catenin. In addition, WIF1 expression decreases the phosphorylation levels of phospho-GSK3β at Ser^9. These results provide evidence that WIF1 expression inhibits the Wnt/β-catenin pathway in T24 and TSU-PR1 cells. In addition, WIF1 expression is associated with down-regulation of two cell cycle regulators: c-myc and SKP2 (Fig. 2D). c-myc is a putative Wnt target gene and a repressor for p21 transcription (25) and SKP2 is a E3 ubiquitin ligase responsible for regulation of p27 protein degradation (34). Thus, p21 and p27 accumulation by WIF1 expression (Fig. 2B) may be due to the inhibition of Wnt signaling-mediated c-*myc* and *SKP2* gene transcription. Together, our data suggest that WIF1 binds to Wnt1 for inhibition of Wnt1/β-catenin pathway, which leads to down-regulation of specific cell cycle-related Wnt target genes for G_1 arrest and decreased cell growth.

Inhibition of Nuclear Wnt Signaling by DN-LEF1 or by shRNA Knockdown of TCF4 Decreases SKP2 Expression Leading to Cell Growth Inhibition

To examine whether inhibition of Wnt signaling in the nucleus results in effects similar to Wnt inhibition by WIF1 at the membrane, we have constructed a DN-LEF1 expression plasmid for inhibition of TCF4/LEF1- and β-catenin-mediated transcription (30). We have successfully established stable TSU-PR1 cell clones expressing DN-LEF1 mRNA (Fig. 3A, *inset*). Figure 3A and B show that TSU-PR1 cells stably transfected with DN-LEF1 exhibit a significantly lower rate of anchorage-dependent and anchorage-independent growth than those transfected with pRK5 at the end of experiments (P values < 0.01, Student's t test). Consistent with the results of WIF1 described above (Fig. 2B and D), the growth-inhibitory effect of DN-LEF1 on TSU-PR1 cells was associated with down-regulation of c-myc and SKP2 and up-regulation of the CDK inhibitors: p21 and p27 (Fig. 3C). These results strongly suggest that WIF1-mediated cell growth inhibition and cell cycle regulation may be involved in transcriptional regulation by nuclear Wnt signaling.

In addition, we stably transfected four shRNA constructs, targeting different exons of TCF4, into TSU-PR1 cells. Two

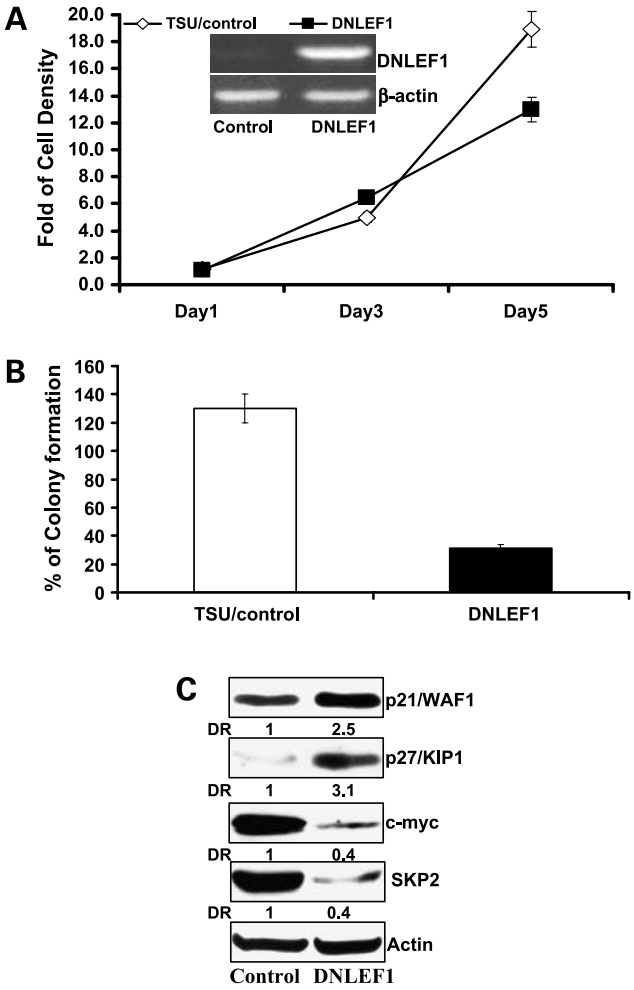

Figure 3. Inhibition of Wnt signaling in TSU-PR1 cells by DN-LEF1 decreases anchorage-dependent and anchorage-independent growth via alteration of cell cycle regulation. **A,** cell proliferation assay in TSU-PR1 cells expressing control or DN-LEF1 at 1, 3, and 5 d after cell seeding. *Inset,* total RNA was extracted and reverse transcription-PCR analysis of *DN-LEF1* mRNA in TSU-PR1 cells expressing DN-LEF1 or transfected with control vector as described in Materials and Methods. **B,** quantitative analysis of soft agar colony formation in TSU-PR1 cells expressing DN-LEF1 or transfected with control vector. *Columns,* mean of four independent wells at optimum time of 21 d after the start of cell seeding; *bars,* SE. **C,** Western blotting analysis of p27/Kip1, p21/WAF1, c-myc, and SKP2 protein expression in TSU-PR1 cells expressing DN-LEF1 or transfected with control vector. Membranes were ''stripped'' and reprobed with anti-actin antibody for determination of protein loading control. Representative of three independent experiments.

constructs (named as shTCF4 C and D) that successfully knocked down the protein expression of TCF4 by 75% to 90% were chosen for further studies (Supplementary Fig. S1B).[6] Consistently, knockdown of TCF4 expression by shRNA caused cell growth inhibition and down-regulation

[6] Supplementary material for this article is available at Molecular Cancer Therapeutics Online (http://mct.aacrjournals.org/).

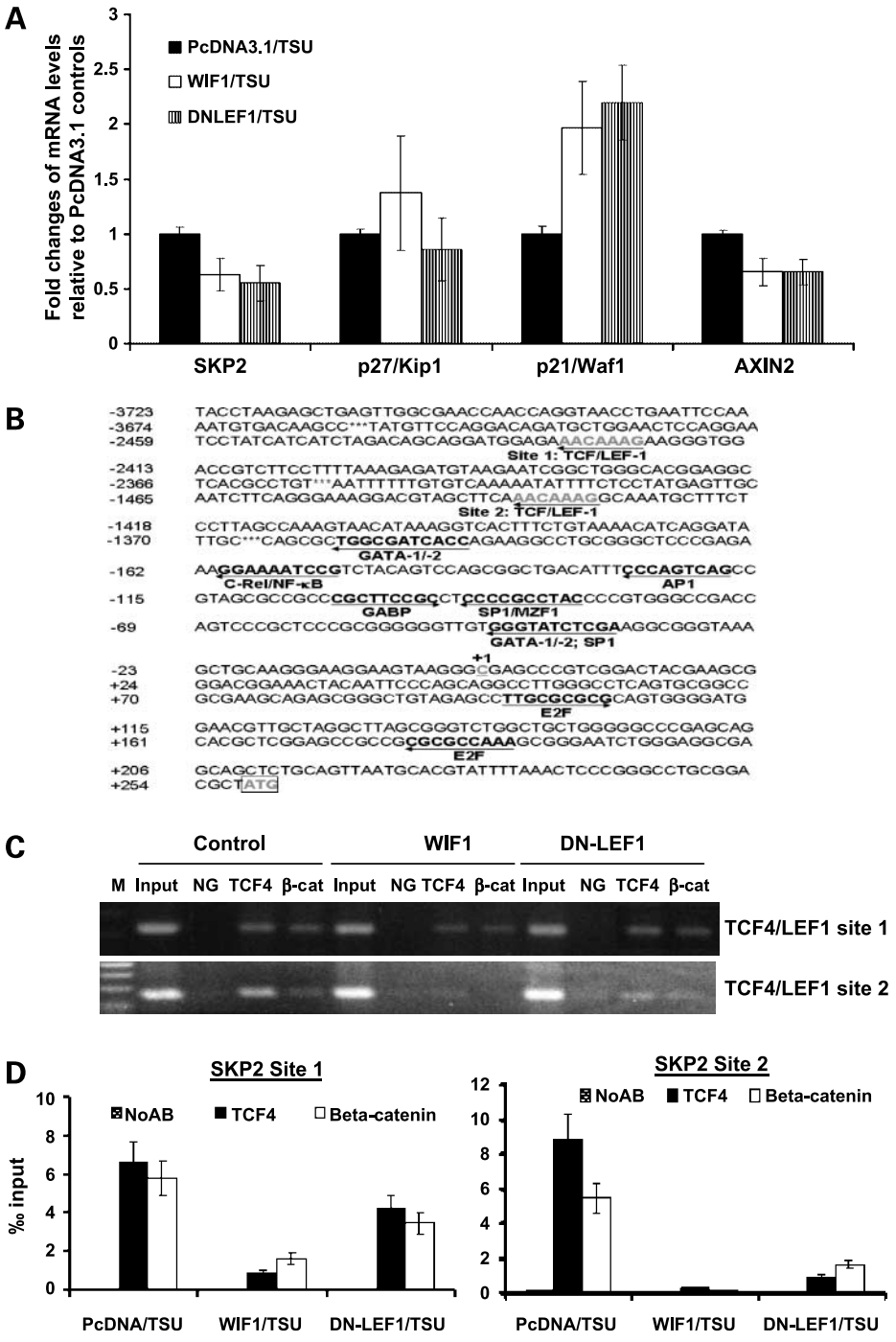

Figure 4. Ectopic expression of WIF1 or DN-LEF1 in TSU-PR1 cells inhibits TCF4 and β-catenin binding to SKP2 promoter sequences. **A,** real-time RT-PCR analysis of *p21, p27*, and *SKP2* mRNA of stable WIF1 or DN-LEF1 transfectants in TSU-PR1 cells as mentioned in Materials and Methods. β-Actin was determined as a loading control. **B,** partial nucleotide sequence of human *SKP2* gene promoter. The transcriptional start site (*+1*) and the potential TCF4/LEF1, GATA, nuclear factor-κB, AP-1, GABP, and E2F binding sites are *underlined*. **C,** chromatin immunoprecipitation assay as described in Materials and Methods. Chromatin immunoprecipitation using anti-TCF4 and anti-β-catenin antibodies was done in TSU-PR1 cells. Eluted DNA fragments were purified and used for PCR using primers specific for the SKP2 proximal promoter. TCF/LEF binding elements are composed of a highly conserved consensus sequence 5′-(A/T)(A/T)CAA(A/T)G-3′. *Input,* 1:20 reversal cross-link chromatin DNA; *NG,* negative control without antibody. **D,** chromatin immunoprecipitation/real-time PCR assay as described in Materials and Methods. The chromatin immunoprecipitation results obtained by three independent replicate experiments are represented as percentage of input. *Bars,* SE. *Black* and *white bars,* chromatin immunoprecipitation signals; *grid bars,* signals from the no antibody control (*NoAb*).

of SKP2 protein expression in TSU-PR1 cells (Supplementary Fig. S1A and B)[6] similar to the effects of DN-LEF1. Together, these results suggest a potential role of SKP2 as a Wnt target gene.

Ectopic Expression of WIF1 or DN-LEF1 in TSU-PR1 Cells Decreases SKP2 mRNA Transcription via Inhibition of TCF4 and β-Catenin Binding to SKP2 Promoter

Using real-time PCR analysis, we observed that stable transfection of WIF1 or DN-LEF1 in TSU-PR1 cells is associated with down-regulation of a known Wnt target gene *AXIN2* and *SKP2* mRNA expression and up-regulation of *p21* mRNA levels (P values < 0.05, Student's t test; Fig. 4A). However, there is no significant change in mRNA expression of p27 in these WIF1 or DN-LEF1 transfectants (P values > 0.05, Student's t test; Fig. 4A). The down-regulation of *AXIN2* gene expression in general indicates inhibition of the Wnt/β-catenin signaling in these WIF1- or DN-LEF1-expressing cells (32).

Given that inhibition of Wnt signaling by either WIF1 or DN-LEF1 expression down-regulates *SKP2* mRNA expression (Fig. 4A), we reasoned that *SKP2* gene could be transcriptionally regulated by TCF4 or its cofactor β-catenin. By searching the promoter sequence of *SKP2* in a transcription factor binding site database using Genomatix software, we found two consensus motifs for the TCF4 binding site [(A/T)(A/T)TCAAAG] (Fig. 4B). Furthermore, we tested by chromatin immunoprecipitation whether TCF4 or β-catenin can bind to the *SKP2* promoter sequence and whether Wnt inhibitors WIF1 and DN-LEF1 can inhibit the binding of TCF4 or β-catenin to the *SKP2* promoter. Figure 4C shows that TCF4 or β-catenin is constitutively bound to the *SKP2* promoter in TSU-PR1 cells. In contrast, ectopic expression of either WIF1 or DN-LEF1 inhibits the *in vivo* binding of TCF4 and β-catenin to the *SKP2* promoter predominantly through TCF/LEF1 binding site 2, which is closer to the *SKP2* transcription initiation site. Furthermore, real-time PCR was done to quantify the enrichment of TCF/LEF1 binding site sequences in the TCF4- and β-catenin-bound DNA from transfected cells. Figure 4D shows that the enrichment of TCF/LEF1 binding site 1 in TCF4- and β-catenin-bound DNA is ~0.64% and 0.59% relative to input, respectively, and the enrichment of TCF/LEF1 binding site 2 in TCF4- and β-catenin-bound DNA is ~0.85% and 0.58% relative to input, respectively, from control transfected TSU-PR1 cells. However, the yield of TCF/LEF1 binding site 1 sequences in the TCF4- and β-catenin-bound DNA was only 0.15% and 0.17% relative to input from WIF1-transfected cells (P values < 0.05, Student's t test) and 0.4% and 0.37% relative to input in DN-LEF1-transfected cells (P values > 0.05, Student's t test), respectively. The yield of TCF/LEF1 binding site 2 sequences in the TCF4- and β-catenin-bound DNA was only 0.02% and 0.01% from WIF1-transfected cells and 0.1% and 0.15% in DN-LEF1-transfected cells, respectively (P values < 0.01, Student's t test).

In addition, Supplementary Fig. S2[6] shows that ectopic expression of SKP2 in WIF1-overexpressing TSU-PR1 cells results in ~10% decrease in G_1 population accompanying by an increase in S and G_2-M population (P values < 0.05,

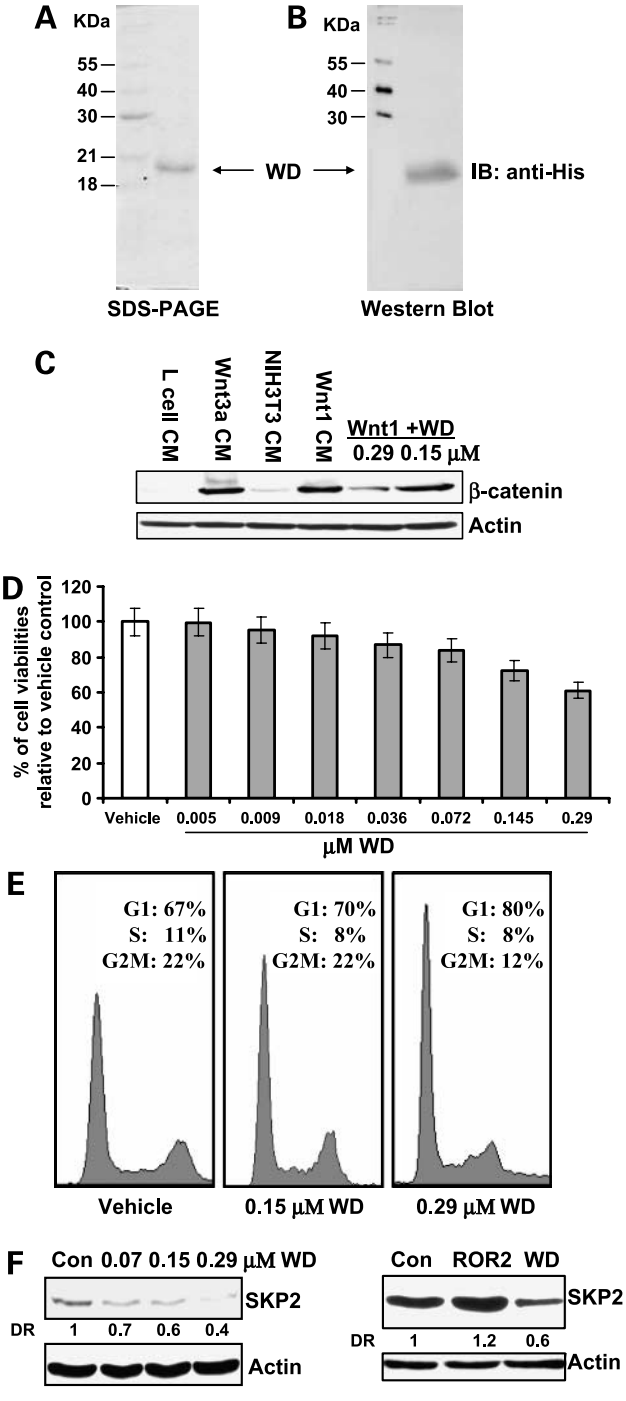

Figure 5. Recombinant WD protein inhibits Wnt1-mediated signaling and cell growth via G_1 arrest and down-regulation of SKP2. **A** and **B,** expression and purification of recombinant WD protein (amino acids 27-176) in *E. coli* by Ni-NTA chromatography and gel filtration as detailed in Materials and Methods. The recombinant WD protein was induced with 1 mmol/L IPTG at 37°C and the refolded WD protein was purified by nickel column chromatography with an imidazole gradient elution (20-500 mmol/L) and gel filtration on HiLoad 16/60 Superdex 75 column chromatography. Purified WD was subjected to SDS-PAGE and Western blot analysis to verify the protein. Membrane was probed for anti-His antibody. **C,** effect of the recombinant WD protein on the Wnt/β-catenin pathway in mouse fibroblast L cells. L cells were treated with Wnt1 and Wnt3a conditioned medium and recombinant WD for 3 h. The cell lysates were prepared and Western blotting was done using anti-β-catenin antibody. **D,** effect of the recombinant WD protein on cell proliferation in T24 cells. Cells (2×10^4) were plated in 24-well culture plates and treated 48 h with different concentrations from 4.53 nmol/L to 0.29 μmol/L. The cell viabilities were measured by 3-(4,5-dimethylthiazol-2-yl)-2,5-diphenyltetrazolium bromide assays. $P < 0.05$ at the concentrations of 0.145 and 0.29 μmol/L recombinant WD protein. *Bars,* SD. **E,** effect of the recombinant WD protein on cell cycle distribution in T24 cells. T24 cells were treated with WD buffer (control) or 0.145 and 0.29 μmol/L WD for 48 h and cell cycle distribution was analyzed by flow cytometry as detailed in Materials and Methods. **F,** effect of the recombinant WD protein on SKP2 protein expression in T24 cells. T24 cells were treated with 0.07, 0.145, and 0.29 μmol/L WD or 0.29 μmol/L recombinant ROR2 proteins for 48 h and the SKP2 protein expression was determined by Western blotting as detailed in Materials and Methods.

Student's *t* test). Together, these results suggest that Wnt signaling engages cell cycle regulation, at least in part, through transcriptional regulation of SKP2.

Recombinant WD Protein Inhibits Wnt Signaling and Cell Growth via G_1 Arrest and Down-Regulation of SKP2

To test the effect of WIF1 on bladder cancer cells in a physiologically relevant manner, we have used a recombinant WD protein produced in *E. coli*. Figure 5A and B show the homogeneity of purified WD protein, which migrates as a protein of the expected molecular weight of ~20 kDa. We next examined the ability of this recombinant WD protein to inhibit Wnt-mediated signaling. Mouse fibroblast L cells do not express cadherins or sequester β-catenin into membrane-bound fractions. Therefore, L cells and Western analysis of total β-catenin provide a convenient method to monitor canonical Wnt signaling and the inhibitory effect of added factors (35). Figure 5C shows that treatment with conditioned medium containing Wnt1 and Wnt3a for 3 h caused a significant accumulation of β-catenin in L cells. Conversely, addition of WD, to 0.29 μmol/L, in combination with Wnt1- and Wnt3a-containing conditioned medium resulted in an inhibition of Wnt1- and Wnt3a-induced β-catenin accumulation (Fig. 5C).

Further, we observed that addition of WD leads to the inhibition of the growth of T24 cells in a dose-dependent manner (Fig. 5D). At 0.29 μmol/L concentration, WD protein inhibits the growth of T24 cells by 40% ($P < 0.05$, Student's *t* test). Moreover, Fig. 5E shows that the growth-inhibitory effect of WD protein on T24 cells was associated with a G_1 arrest (G_1 populations for vehicle control versus 0.145 or 0.29 μmol/L recombinant WD protein are 67% versus 70% or 80%; *P* values < 0.05, Student's *t* test). Western analysis also reveals that recombinant WD protein significantly decreased the SKP2 protein level in a dose-dependent manner, whereas another recombined protein, ROR2, obtained by similar method as WD protein, did not reduce the SKP2 protein expression (Fig. 5F). This result suggests the specificity of recombinant WD protein in down-regulation of SKP2 expression in T24 cells. The sum of results indicates that inhibition of the Wnt/β-catenin pathway and attenuation of cell growth by WIF1 are physiologically relevant.

WIF1 Inhibits *In vivo* Tumor Growth of TSU-PR1 Cells in a Xenograft Mouse Model

Figure 6A shows that the ectopic expression of WIF1 in TSU-PR1 cells results in a significant decrease in the growth rate of tumors compared with control ($P < 0.01$, ANOVA). The wet tumor weights in control and WIF1 transfectant group recorded at the end of the treatment were 616.5 ± 272 and 316.17 ± 259 mg, respectively (Fig. 6B; $n = 10$, mean ± SD; $P < 0.05$, Student's *t* test). Ectopic WIF1 expression attenuated tumor growth by 58%. Immunohistochemical analysis using an anti-WIF1 antibody confirms WIF1 protein expression in tumors from WIF1-transfected cell line but not in tumor from vector control cell lines (Fig. 6C).

Discussion

The reported molecular mechanisms for regulation of the G_1-S transition by Wnt signaling include (*a*) its direct regulation of *cyclin D1* transcription (29) and (*b*) its indirect control of p21 expression via targeting *c-myc* transcription (25). The present study provides the first evidence to support the notion that Wnt signaling also requires regulation of SKP2, the F-box subunit of the ubiquitin-ligase complex SCF^{SKP2}/p27 degradation pathway, for Wnt signaling-mediated G_1-S transition in human urinary bladder cancer cells. The link between Wnt signaling and SKP2 is based on the following findings: the promoter sequence of *SKP2* contains the consensus motif [(A/T)(A/T)TCAAAG] for the TCF/LEF binding site; inhibition of Wnt signaling either by WIF1 at the membrane level or by a DN-LEF1 or knockdown of TCF4 by shRNA at the nuclear level down-regulates *SKP2* mRNA and protein expression and decreases the *in vivo* binding of TCF4/β-catenin to the *SKP2* promoter sequence. Treatment of bladder cancer T24 cells with functional recombinant WD protein also results in a decrease of SKP2 protein expression. Conversely, enhancing Wnt signaling by overexpression of Wnt coreceptor LRP5 in prostate cancer 22Rv1 cells increases the expression of SKP2.[7] Taken together, these results indicate that SKP2 is a potential target of Wnt regulation in several human cancer cells.

Accumulating evidence suggest that SKP2 is an important oncoprotein (34). Frequent amplification of the *SKP2* gene has been detected in primary lung cancers and in cell lines expressing high-risk human papillomavirus (36, 37). Pathways like phosphatidylinositol 3-kinase, nuclear factor-κB, and Notch signaling have been shown to regulate *SKP2* transcription (38). In addition, several potential regulatory elements have been identified in the promoter sequence of SKP2, including binding sites for transcription factors c-Rel/nuclear factor-κB, AP-1, SRY, Sp1, GATA, FOXP3, and E2F (38–42). Notably, the potential Wnt target gene *SKP2* and the confirmed Wnt target *c-myc* (25) are the direct targets of the Notch signaling (42). Because c-myc acts as a transcription repressor for p21 gene expression (25) and p27 protein is a major physiologic target for SKP2-mediated degradation (34, 39), there is a striking similarity between Notch and Wnt signaling in terms of p21 and p27 regulation and for the regulation of a proliferation/differentiation balance. Given that multiple transcriptional factors can bind to the promoter sequence of *SKP2*, we can speculate that Wnt signaling may act cooperatively with other developmental pathways (e.g., Notch pathway; ref. 43) or growth factor pathways (e.g., AP-1) to regulate SKP2 transcription, leading to a cell type-specific proliferation in G_1 as described in its regulation of stem and progenitor cells (25). Thus, our results argue that Wnt signaling regulating the SKP2/p27 degradation pathway

[7] Y. Tang et al., unpublished data.

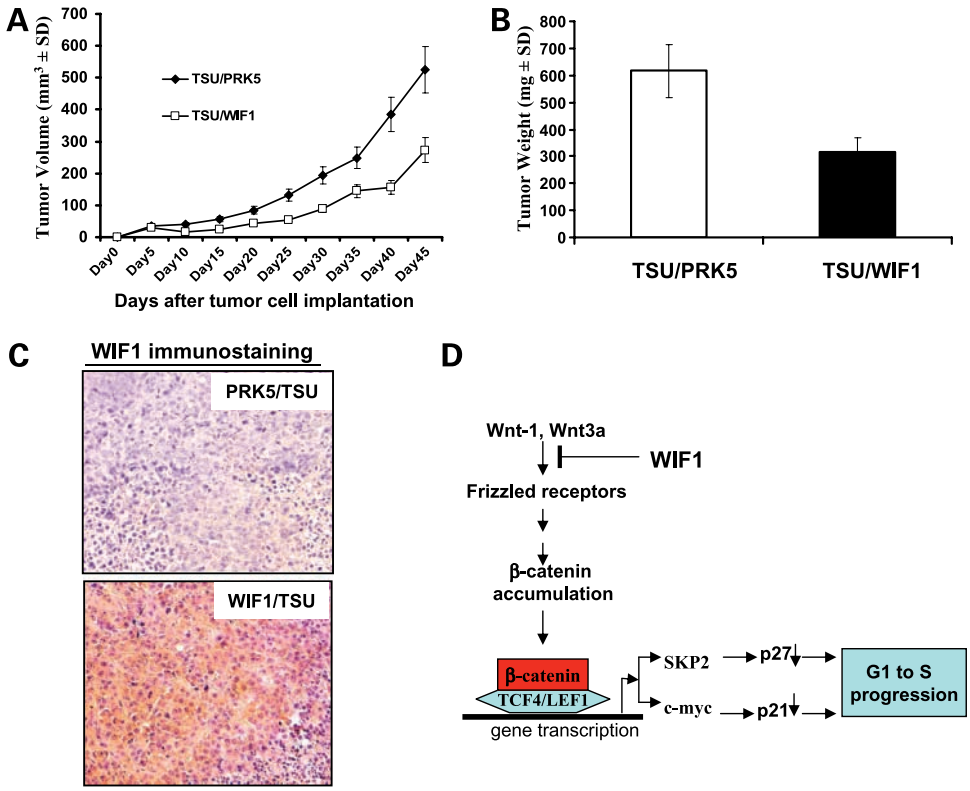

Figure 6. Ectopic expression of WIF1 in TSU-PR1 cells inhibits tumor growth in a xenograft model. TSU-PR1 cells (2×10^6) stably transfected with pRK5 control or WIF1 were injected into the left flank of NCR-*nu/nu* (nude) mice. **A,** *points,* mean tumor volume (each group contains 10 mice); *bars,* SE. **B,** at the termination of the study on day 50, tumors were excised from each mouse in different groups and weighed. Wet weight of tumors is represented as mean of 10 tumors from individual mouse in each group. $P < 0.05$ at the termination of the experiments. *Bars,* SE. **C,** immunohistochemical staining of ectopic WIF1 expression (with anti-WIF1 antibody) in harvested mouse tumor samples. **D,** model of a mechanism by which WIF-1 induces G_1 arrest. WIF-1 inhibits Wnt/β-catenin- and TCF4/LEF1-mediated transcription of cell cycle-related genes (*SKP2* and *c-myc*), leading to up-regulation of p27 and p21 followed by G_1 arrest.

may be physiologically relevant in bladder cancer. This testable hypothesis will need to be further studied.

We show here that WIF1 expression exhibited significant cell and tumor growth-inhibitory effects on human urinary bladder cancer cell lines. This result is consistent with recent reports that overexpression of WIF1 inhibits the growth of multiple other cancer cell lines (13–24). Moreover, the use of recombinant WD protein in this study has allowed us to rule out the possibility that nonphysiologically relevant secondary factors produced by WIF1-expressing cells in the cultures were the source of the observed growth-inhibitory effects of WIF1. Among Wnt family members, Wnt1 and Wnt3a are known to be essential growth factors in small intestine, colon tissues, and stem cells (44, 45). The three-dimensional structure of the WD protein determined by nuclear magnetic resonance spectroscopy suggests that the WD recognizes and binds to Wnts via palmitoylation and that the recognition of palmitoylated Wnts by WIF1 is affected by its WD rather than by its epidermal growth factor domains (46). We show here that WIF1 fusion protein can form an immunocomplex with Wnt1 in cell cultures and that WD protein inhibits both Wnt1- and Wnt3a-containing conditioned medium-mediated β-catenin accumulation. In addition, the inhibition of Wnt-mediated growth effect on bladder cancer cells by expression of WIF1 is associated with inhibition of the β-catenin-mediated cell proliferation. This is evidenced by an activation of GSK3β, by a decrease in the cytosolic β-catenin levels, and by a reduction in TCF4-mediated transcription of cell cycle-related genes (e.g., *c-myc* and *SKP2*). Conversely, Urakami et al. (7) showed that suppression of WIF1 expression by small interfering RNA in the bladder cancer cell line, UMUC, up-regulated the expression of Wnt target genes including *c-myc* and *cyclin D1* and accelerated cell growth. Taken together, these results provide strong evidence that the mechanisms for WIF1-inhibiting bladder cancer cell growth is associated with its inhibition of Wnt-mediated and β-catenin-dependent transcription of cell cycle-related Wnt target genes.

In summary, our data are consistent with the model shown in Fig. 6D. The antiproliferative effect of WIF1 on bladder cancer cells is associated with its inhibition of Wnt/β-catenin-mediated transcription of cell cycle-regulating genes (*c-myc* and *SKP2*). The down-regulation of c-myc and SKP2 then results in accumulation of p21/WAF1 and p27/Kip1, which bind to and inhibit CDK2 kinase, thereby inhibiting cell growth. In addition, we show that WIF1 decreases *SKP2* gene transcription by inhibiting the *in vivo* binding of TCF4 and β-catenin to the *SKP2* promoter. For the first time, these results suggest that *SKP2* is a potentially important target gene for the Wnt/β-catenin-regulated G_1-S transition. Therefore, our results have provided new information for understanding mechanisms of bladder cancer pathogenesis, which may facilitate development of novel target agents for bladder cancer therapy and prevention.

Disclosure of Potential Conflicts of Interest

No potential conflicts of interest were disclosed.

Acknowledgments

We thank Dr. Jen-Chih Hsieh for the *WIF1* construct, Dr. Andrew P. McMahon for NIH3T3/Wnt1 cell line, and Dr. Marian Waterman for advices and technical support.

References

1. Cookson MS, Herr HW, Zhang ZF, Soloway S, Sogani PC, Fair WR. The treated natural history of high risk superficial bladder cancer: 15-year outcome. J Urol 1997;158:62 – 7.

2. Snyder C Harlan L, Knopf K, Potosky A, Kaplan R. Patterns of care for the treatment of bladder cancer. J Urol 2003;169:1697 – 701.

3. Moon RT, Kohn AD, De Ferrari GV, Kaykas A. Wnt and β-catenin signalling: diseases and therapies. Nat Rev Genet 2004;5:691 – 701.

4. Shiina H, Igawa M, Shigeno K, et al. β-Catenin mutations correlate with over expression of c-Myc and cyclin D1 genes in bladder cancer. J Urol 2002;168:2220 – 6.

5. Stoehr R, Krieg RC, Knuechel R, et al. No evidence for involvement of β-catenin and APC in urothelial carcinomas. Int J Oncol 2002;20:905 – 11.

6. Urakami S, Shiina H, Enokida H, et al. Combination analysis of hypermethylated Wnt-antagonist family genes as a novel epigenetic biomarker panel for bladder cancer detection. Clin Cancer Res 2006;12: 2109 – 16.

7. Urakami S, Shiina H, Enokida H, et al. Epigenetic inactivation of Wnt inhibitory factor-1 plays an important role in bladder cancer through aberrant canonical Wnt/β-catenin signaling pathway. Clin Cancer Res 2006;12:383 – 91.

8. Marsit CJ, Karagas MR, Andrew A, et al. Epigenetic inactivation of SFRP genes and TP53 alteration act jointly as markers of invasive bladder cancer. Cancer Res 2005;65:7081 – 5.

9. Stoehr R, Wissmann C, Suzuki H, et al. Deletions of chromosome 8p and loss of sFRP1 expression are progression markers of papillary bladder cancer. Lab Invest 2004;84:465 – 78.

10. Marsit CJ, McClean MD, Furniss CS, Kelsey KT. Epigenetic inactivation of the SFRP genes is associated with drinking, smoking and HPV in head and neck squamous cell carcinoma. Int J Cancer 2006;119: 1761 – 6.

11. Abdel-Aziz HO, Takasaki I, Tabuchi Y, et al. High-density oligonucleotide microarrays and functional network analysis reveal extended lung carcinogenesis pathway maps and multiple interacting genes in NNK [4-(methylnitrosamino)-1-(3-pyridyle)-1-butanone] induced CD1 mouse lung tumor. J Cancer Res Clin Oncol 2007;133:107 – 15.

12. Hsieh JC, Kodjabachian L, Rebbert ML, et al. A new secreted protein that binds to Wnt proteins and inhibits their activities. Nature 1999;398: 431 – 6.

13. Batra S, Shi Y, Kuchenbecker KM, et al. Wnt inhibitory factor-1, a Wnt antagonist, is silenced by promoter hypermethylation in malignant pleural mesothelioma. Biochem Biophys Res Commun 2006;342:1228 – 32.

14. Taniguchi H, Yamamoto H, Hirata T, et al. Frequent epigenetic inactivation of Wnt inhibitory factor-1 in human gastrointestinal cancers. Oncogene 2005;24:7946 – 52.

15. Reguart N, He B, Xu Z, et al. Cloning and characterization of the promoter of human Wnt inhibitory factor-1. Biochem Biophys Res Commun 2004;323:229 – 34.

16. Mazieres J, He B, You L, et al. Wnt inhibitory factor-1 is silenced by promoter hypermethylation in human lung cancer. Cancer Res 2004;64: 4717 – 20.

17. Elston MS, Gill AJ, Conaglen JV, et al. Wnt pathway inhibitors are strongly down-regulated in pituitary tumors. Endocrinology 2008;149: 1235 – 42.

18. Lin YC, You L, Xu Z, et al. Wnt inhibitory factor-1 gene transfer inhibits melanoma cell growth. Hum Gene Ther 2007;18:379 – 86.

19. Queimado L, Lopes CS, Reis AM. WIF1, an inhibitor of the Wnt pathway, is rearranged in salivary gland tumors. Genes Chromosomes Cancer 2007;46:215 – 25.

20. Chim CS, Chan WW, Pang A, Kwong YL. Preferential methylation of Wnt inhibitory factor-1 in acute promyelocytic leukemia: an independent poor prognostic factor. Leukemia 2006;20:907 – 9.

21. Ai L, Tao Q, Zhong S, et al. Inactivation of Wnt inhibitory factor-1 (WIF1) expression by epigenetic silencing is a common event in breast cancer. Carcinogenesis 2006;27:1341 – 8.

22. Wissmann C, Wild PJ, Kaiser S, et al. WIF1, a component of the Wnt pathway, is down-regulated in prostate, breast, lung, and bladder cancer. J Pathol 2003;201:204 – 12.

23. Yamashita S, Tsujino Y, Moriguchi K, Tatematsu M, Ushijima T. Chemical genomic screening for methylation-silenced genes in gastric cancer cell lines using 5-aza-2′-deoxycytidine treatment and oligonucleotide microarray. Cancer Sci 2006;97:64 – 71.

24. Ohigashi T, Mizuno R, Nakashima J, Marumo K, Murai M. Inhibition of Wnt signaling downregulates Akt activity and induces chemosensitivity in PTEN-mutated prostate cancer cells. Prostate 2005;62:61 – 8.

25. van de Wetering M, Sancho E, Verweij C, et al. The β-catenin/TCF-4 complex imposes a crypt progenitor phenotype on colorectal cancer cells. Cell 2002;111:241 – 50.

26. Jho EH, Zhang T, Domon C, Joo CK, Freund JN, Costantini F. Wnt/β-catenin/Tcf signaling induces the transcription of Axin2, a negative regulator of the signaling pathway. Mol Cell Biol 2002;22:1172 – 83.

27. Pfeuty B, David-Pfeuty T, Kaneko K. Underlying principles of cell fate determination during G_1 phase of the mammalian cell cycle. Cell Cycle 2008;7:3246 – 57.

28. Li Y, Hively WP, Varmus HE. Use of MMTV-Wnt-1 transgenic mice for studying the genetic basis of breast cancer. Oncogene 2000;19:1002 – 9.

29. Tetsu O, McCormick F. β-Catenin regulates expression of cyclin D1 in colon carcinoma cells. Nature 1999;398:422 – 6.

30. Zi X, Guo Y, Simoneau AR, et al. Expression of Frzb/secreted Frizzled-related protein 3, a secreted Wnt antagonist, in human androgen-independent prostate cancer PC-3 cells suppresses tumor growth and cellular invasiveness. Cancer Res 2005;65:9762 – 70.

31. Zi X, Zhang J, Agarwal R, Pollak M. Silibinin up-regulates insulin-like growth factor-binding protein 3 expression and inhibits proliferation of androgen-independent prostate cancer cells. Cancer Res 2000;60: 5617 – 20.

32. Collins I, Garrett MD. Targeting the cell division cycle in cancer: CDK and cell cycle checkpoint kinase inhibitors. Curr Opin Pharmacol 2005;5: 366 – 73.

33. Lu W, Yamamoto V, Ortega B, Baltimore D. Mammalian Ryk is a Wnt coreceptor required for stimulation of neurite outgrowth. Cell 2004;119: 97 – 108.

34. Gstaiger M, Jordan R, Lim M, et al. Skp2 is oncogenic and overexpressed in human cancers. Proc Natl Acad Sci U S A 2001;98: 5043 – 8.

35. Galli LM, Barnes T, Cheng T, et al. Differential inhibition of Wnt-3a by Sfrp-1, Sfrp-2, and Sfrp-3. Dev Dyn 2006;235:681 – 90.

36. Dowen SE, Neutze DM, Pett MR, et al. Amplification of chromosome 5p correlates with increased expression of Skp2 in HPV-immortalized keratinocytes. Oncogene 2003;22:2531 – 40.

37. Yokoi S, Yasui K, Saito-Ohara F, et al. A novel target gene, SKP2, within the 5p13 amplicon that is frequently detected in small cell lung cancers. Am J Pathol 2002;161:207 – 16.

38. Huang YC, Hung WC. 1,25-Dihydroxyvitamin D_3 transcriptionally represses p45Skp2 expression via the Sp1 sites in human prostate cancer cells. J Cell Physiol 2006;209:363 – 9.

39. Nakayama K, Ishida N, Shirane M, et al. Mice lacking p27(Kip1) display increased body size, multiple organ hyperplasia, retinal dysplasia, and pituitary tumors. Cell 1996;85:707 – 20.

40. Zhang L, Wang C. F-box protein Skp2: a novel transcriptional target of E2F. Oncogene 2006;25:2615 – 27.

41. Zuo T, Liu R, Zhang H, et al. FOXP3 is a novel transcriptional repressor for the breast cancer oncogene SKP2. J Clin Invest 2007;117: 3765 – 73.

42. Sarmento LM, Huang H, Limon A, et al. Notch1 modulates timing of G_1-S progression by inducing SKP2 transcription and p27 Kip1 degradation. J Exp Med 2005;202:157 – 68.

43. Herranz H, Pérez L, Martín FA, Milán M. A Wingless and Notch double-repression mechanism regulates G_1-S transition in the *Drosophila* wing. EMBO J 2008;27:1633 – 45.

44. Hoffman J, Kuhnert F, Davis CR, Kuo CJ. Wnts as essential growth factors for the adult small intestine and colon. Cell Cycle 2004;3:554 – 7.

45. Willert K, Brown JD, Danenberg E, et al. Wnt proteins are lipid-modified and can act as stem cell growth factors. Nature 2003;423:448 – 52.

46. Liepinsh E, Banyai L, Patthy L, Otting G. NMR structure of the WIF domain of the human Wnt-inhibitory factor-1. J Mol Biol 2006;357:942 – 50.